Contribution from Rocketdyne, A Division of Rockwell International, Canoga Park, California 91304, the Centre d'Etudes Nucleaires de Saclay, 91191 Gif-sur-Yvette Cedex, France, and the Department of Chemistry, University of Leicester, Leicester LEI 7RH, U.K.

Structure and Vibrational Spectra of Oxonium Hexafluoroarsenates(V) and -antimonates(V)

K. O. CHRISTE,*[1] P. CHARPIN,[2] E. SOULIE,[2] R. BOUGON,[2] J. FAWCETT,[3] and D. R. RUSSELL[3]

Received February 28, 1984

The salts $OD_3^+AsF_6^-$, $OD_3^+SbF_6^-$, and partially deuterated $OH_3^+SbF_6^-$ were prepared and characterized by X-ray and neutron diffraction techniques, DSC measurements, and vibrational spectroscopy. At room temperature, $OH_3^+AsF_6^-$ exists in a plastic phase where ions, centered on the atomic positions of the NaCl structure, are in motion or oscillation. No valuable information on atomic distances or angles in $OH_3^+AsF_6^-$ could be obtained due to these dynamic structural disorder problems. For $OH_3^+SbF_6^-$ the phase transition from an ordered to a disordered phase was shown to occur above room temperature. The room-temperature phase can be described by an ordered hydrogen-bonded model based on a CsCl type structure. Vibrational spectra were recorded for these oxonium salts and confirm the presence of the different phases and phase transitions. Improved assignments are given for the OH_3^+ and OD_3^+ cations, and the OH···FM bridge stretching mode and some of the bands characteristic for OD_2H^+ and ODH_2^+ were identified. A modified valence force field was calculated for OH_3^+, which is in good agreement with the known general valence force field of isoelectronic NH_3 and values obtained by ab initio calculations. From the OH···FM stretching mode, the hydrogen-bridge bond strength was found to be 1.77 kcal mol^{-1}.

Introduction

Although the existence of oxonium salts at low temperature had been well known for many years, the synthesis of surprisingly stable OH_3^+ salts containing the AsF_6^- and SbF_6^- anions has been reported[4] only in 1975. Since then, numerous papers have been published on other OH_3^+ salts containing complex fluoro anions such as UF_6^-,[5] BiF_6^-,[6] IrF_6^-, PtF_6^-, RuF_6^-,[7,8] TiF_5^-,[9] or BF_4^-.[10] In these oxonium salts the cations and anions are strongly hydrogen bonded, as shown by the short O-F distances of 2.51-2.61 Å found by X-ray diffraction studies.[9,10] Since the nature of these hydrogen bridges is strongly temperature dependent, these oxonium salts show phase transitions and present interesting structural problems. In this paper we report unpublished results accumulated during the past 8 years in our laboratories for these oxonium salts.

Experimental Section

Materials and Apparatus. Volatile materials used in this work were manipulated in a well-passivated (with ClF_3 and HF or DF) Monel Teflon FEP vacuum system.[11] Nonvolatile materials were handled in the dry-nitrogen atmosphere of a glovebox. Hydrogen fluoride (Matheson Co.) was dried by storage over BiF_5.[6] SbF_5 and AsF_5 (Ozark Mahoning Co.) were purified by distillation and fractional condensation, respectively, and DF (Ozark Mahoning Co.) and D_2O (99.6%, Volk) were used as received. Literature methods were used for the preparation of O_2AsF_6,[12] OH_3SbF_6, and OH_3AsF_6.[4]

Infrared spectra were recorded on a Perkin-Elmer Model 283 spectrometer, which was calibrated by comparison with standard gas calibration points.[13,14] Spectra of solids were obtained by using dry powders pressed between AgCl or AgBr windows in an Econo press (Barnes Engineering Co.). For low-temperature spectra, the pressed silver halide disks were placed in a copper block cooled to -196 °C with liquid N_2 and mounted in an evacuated 10-cm path length cell equipped with CsI windows.

Raman spectra were recorded on a Cary Model 83 spectrophotometer using the 4880-Å exciting line and a Claassen filter[15] for the elimination of plasma lines. Sealed quartz tubes were used as sample containers in the transverse-viewing, transverse-excitation technique. The low-temperature spectra were recorded with a previously described[16] device.

A Perkin-Elmer differential-scanning calorimter, Model DSC-1B, equipped with a liquid-N_2-cooled low-temperature assembly, was used to measure phase transitions above -90 °C. The samples were crimp sealed in aluminum pans, and a heating rate of 5°/min in N_2 was used. The instrument was calibrated with the known melting points of *n*-octane, water, and indium.

The neutron powder diffraction patterns of $OH_3^+AsF_6^-$, $OD_3^+AsF_6^-$, and $O_2^+AsF_6^-$ were measured at Saclay on the research reactor EL3 with λ = 1.140 Å for 2θ ranging from 6 to 44°. The data for $OD_3^+SbF_6^-$ were recorded at ILL Grenoble with λ = 1.2778 Å for 2θ ranging from 12 to 92° with 400 measured values of intensity separated by 0.10°.

The X-ray powder diffraction patterns were obtained from samples sealed in 0.3-mm Lindemann capillaries with a 114.6-mm diameter Philips camera using Ni-filtered Cu Kα radiation. Low-temperature diagrams were measured with a jet of cold N_2 to cool the sample and a Meric MV3000 regulator.

The single crystal of $OH_3^+SbF_6^-$ was isolated as a side product from the reaction of MoF_4O and SbF_5 in a thin-walled Teflon FEP reactor with H_2O slowly diffusing through the reactor wall.

Preparation of $OD_3^+AsF_6^-$. A sample of D_2O (987.5 mg, 49.30 mmol) was syringed in the drybox into a $^3/_4$-in. Teflon FEP ampule equipped with a Teflon-coated magnetic stirring bar and a stainless-steel valve. The ampule was connected to a Monel Teflon vacuum line, cooled to -196 °C, and evacuated, and DF (10 g) was added. The mixture was homogenized at room temperature, and AsF_5 (57.7 mmol) was added at -196 °C. The mixture was warmed to -78 °C and then to ambient temperature for 1 h with agitation. All material volatile at ambient temperature was pumped off for 2 h, leaving behind a white solid residue (10.408 g; weight calculated for 49.30 mmol of $OD_3^+AsF_6^-$ 10.402 g) identified by IR spectroscopy as mainly $OD_3^+AsF_6^-$ containing a small amount (less than 1%) of $OD_2H^+AsF_6^-$ as impurity.

Preparation of $OD_3^+SbF_6^-$. Antimony pentafluoride (18.448 g, 85.11 mmol) was added in the drybox to a $^3/_4$-in. Teflon FEP ampule equipped with a Teflon-coated magnetic stirring bar and a stainless-steel valve. The ampule was connected to the vacuum line, cooled to -78 °C, and evacuated, and DF (23.1 g) was added. The mixture was homogenized at room temperature. The ampule was cooled inside the drybox to -196 °C, and D_2O (1.6951 g, 84.63 mmol) was added

(1) Rocketdyne.
(2) CEN Saclay.
(3) University of Leicester.
(4) Christe, K. O.; Schack, C. J.; Wilson, R. D. *Inorg. Chem.* **1975**, *14*, 2224.
(5) Masson, J. P.; Desmoulin, J. P.; Charpin, P.; Bougon, R. *Inorg. Chem.* **1976**, *15*, 2529.
(6) Christe, K. O.; Wilson, W. W.; Schack, C. J. *J. Fluorine Chem.* **1978**, *11*, 71.
(7) Selig, H.; Sunder, W. A.; Disalvo, F. A.; Falconer, W. E. *J. Fluorine Chem.* **1978**, *11*, 39.
(8) Selig, H.; Sunder, W. A.; Schilling, F. C.; Falconer, W. E. *J. Fluorine Chem.* **1978**, *11*, 629.
(9) Cohen, S.; Selig, H.; Gut, R. *J. Fluorine Chem.* **1982**, *20*, 349.
(10) Mootz, D.; Steffen, M. *Z. Anorg. Allg. Chem.* **1981**, *482*, 193.
(11) Christe, K. O.; Wilson, R. D.; Schack, C. J. *Inorg. Synth.*, in press.
(12) Shamir, J.; Binenboym, J. *Inorg. Chim. Acta* **1968**, *2*, 37.
(13) Plyler, E. K.; Danti, A.; Blaine, L. R.; Tidwell, E. D. *J. Res. Natl. Bur. Stand., Sect. A* **1960**, *64*, 841.
(14) International Union of Pure and Applied Chemistry. "Tables of Wavenumbers for the Calibration of Infrared Spectrometers"; Butterworths: Washington, D.C., 1961.
(15) Claassen, H. H.; Selig, H.; Shamir, J. *J. Appl. Spectrosc.* **1969**, *23*, 8.
(16) Miller, F. A.; Harney, B. M. *J. Appl. Spectrosc.* **1970**, *24*, 271.

0020-1669/84/1323-3756$01.50/0

with a syringe. The mixture was agitated for several hours at 25 °C, and all material volatile at 45 °C was pumped off for 14 h. The white solid residue (21.987 g; weight calculated for 84.63 mmol of $OD_3^+SbF_6^-$ 21.813 g) was identified by spectroscopic methods as mainly $OD_3^+SbF_6^-$ containing a small amount (less than 1%) of $OD_2H^+SbF_6^-$.

Preparation of Partially Deuterated $OH_3^+SbF_6^-$. A sample of $OH_3^+SbF_6^-$ (2.0016 g, 7.857 mmol) was dissolved in liquid DF (2.012 g, 95.81 mmol) in a Teflon ampule for 1 h. All volatile material was pumped off at 45 °C for 3 h, leaving behind a white solid residue (2.020 g, weight calculated for 7.857 mmol of $OD_3^+SbF_6^-$ 2.0252 g) that on the basis of its vibrational spectra showed about equimolar amounts of OD_3^+ and OD_2H^+ and smaller amounts of $ODH_2^+SbF_6^-$ (calculated statistical product distribution for 19.74% H and 80.26% D (mol %): OD_3^+, 51.68; OD_2H^+, 38.16; ODH_2^+, 9.33; OH_3^+, 0.77).

Results and Discussion

Syntheses and Properties of Deuterated Oxonium Salts. The OD_3^+ salts were prepared by the same method as previously reported[4] for the corresponding OH_3^+ salts, except for replacing H_2O and HF by D_2O and DF, respectively.

$$D_2O + DF + MF_5 \xrightarrow{DF} OD_3^+MF_6^- \qquad M = As, Sb$$

The yields are quantitative, and the samples were almost completely deuterated. The small amounts of OD_2H^+ observed in the infrared spectra and to a lesser degree in the Raman spectra of the products (see below) are attributed to small amounts (0.6%) of H_2O in the D_2O starting material and to exchange with traces of moisture during the preparation of the IR samples. A partially deuterated sample of $OH_3^+SbF_6^-$ was prepared by treating solid $OH_3^+SbF_6^-$ with an excess of DF.

$$OH_3^+SbF_6^- + n\text{DF} \rightarrow OH_{3-n}D_n^+SbF_6^- + n\text{HF}$$

The exchange appeared to be fast, and the product exhibited the correct statistical OD_3^+, OD_2H^+, ODH_2^+, and OH_3^+ distribution based on the H:D ratio of the starting materials. As expected, the physical properties of the deuterated oxonium salts were practically identical with those[4] of the corresponding OH_3^+ salts.

DSC Data. Since the neutron and X-ray diffraction data suggested (see below) that at room temperature OH_3SbF_6 is ordered whereas OH_3AsF_6 exists in a plastic phase, low-temperature DSC data were recorded to locate the corresponding phase changes for each compound.

The OD_3AsF_6 salt exhibited on warm-up from −90 °C a large endothermic phase change at 2.5 °C that was shown to be reversible, occurring at −7.5 °C on cooling. For OH_3AsF_6 this phase change was observed at practically the same temperatures. No other endotherms or exotherms were observed between −90 °C and the onset of irreversible decomposition. The observed phase-change temperatures are in excellent agreement with those found by low-temperature Raman spectroscopy (see below).

For OH_3SbF_6 three small endotherms at 20, 49, and 81 °C and a large endothermic phase change at 100 °C were observed on warming. All of these were reversible, occurring at 19, 42, 77, and 96 °C, respectively, on cooling. For OD_3SbF_6 the corresponding changes were observed at 20, 48, 82, and 100 °C on warming and 20, 43, 74, and 76 °C on cooling. Again no other heat effects were observed in this temperature range. The temperature differences observed for phase changes between the heating and cooling data are attributed to hysteresis, which normally is a problem in salts of this type.[17] The smaller heat effects observed for OH_3SbF_6 below the major order–disorder phase transition may be attributed to damping of rotational motions of the ions, similar to those found for O_2AsF_6.[17]

(17) Griffiths, J. E.; Sunder, W. A. *J. Chem. Phys.* **1982**, *77*, 1087.

Table I. X-ray Diffraction Powder Pattern of OH_3AsF_6 at −153 °C[a]

d_{obsd}, Å	intens	d_{obsd}, Å	intens
6.35	vw	2.024	ms
4.95	s	2.010	m
4.72	s	1.942	m
4.12	w	1.913	vvw
3.87	w	1.877	ms
3.749	ms	1.871	w
3.730		1.802	vw
3.473	m	1.775	vw
3.225	m	1.769	vw
3.163	m	1.739	vw
3.029	mw	1.712	w
2.845	m	1.695	w
2.837		1.659	vw
2.596	w	1.648	mw
2.530	vw	1.612	w
2.362	vvw	1.585	mw
2.139	w	1.581	vw
2.061	m		
2.055			

[a] Cu Kα radiation and Ni filter.

Table II. Neutron Diffraction Powder Patterns of the Face-Centered Cubic, Room-Temperature Phases of OH_3AsF_6, OD_3AsF_6, and O_2AsF_6[a]

	OH_3AsF_6		OD_3AsF_6	O_2AsF_6
hkl	calcd intens	obsd intens	obsd intens	obsd intens
111	1100	1127	12	200
200	177	174	1033	1000
220	11		177	215
311	5		137	210
222	0		19	45
400	2		12	20
331	5			
420	66	71	38	90
422	100	92	26	100
511/333	5		16	35

[a] Intensities in arbitrary units.

For OH_3BiF_6 no phase transitions were observed between −90 °C and the onset of decomposition.

Structural Studies

OH_3AsF_6. As previously reported,[4] this compound is cubic at room temperature, and a cell parameter of 8.043 (8) Å was found in this study from X-ray powder data. It exhibits only one phase transition at −2 ± 5 °C (based on DSC and Raman data) in the temperature range from −90 °C to its decomposition point. The X-ray powder pattern at −153 °C is given in Table I and indicates a lowering of the symmetry in agreement with the low-temperature vibrational spectra (see below). Attempts to index the pattern were unsuccessful.

It is interesting to compare X-ray powder diffraction patterns of OH_3AsF_6 and O_2AsF_6. Whereas their room-temperature patterns[4,12,18] and cell parameters are for practical purposes identical, their low-temperature patterns (Table I and ref 19) are very distinct due to different ion motion freezing. Since OH_3^+, OD_3^+, and O_2^+ are weak X-ray scatterers, but contribute strongly to the neutron scattering, neutron diffraction powder patterns were also recorded at room temperature for their AsF_6^- salts (see Table II). As expected, the cell dimensions were for practical purposes identical, but the observed relative intensities were very different.

Attempts were made to obtain structural information from the room-temperature neutron diffraction powder patterns of

(18) Young, A. R.; Hirata, T.; Morrow, S. I. *J. Am. Chem. Soc.* **1964**, *86*, 20.

(19) Naulin, C.; Bougon, R. *J. Chem. Phys.* **1976**, *64*, 4155.

OH_3AsF_6 and OD_3AsF_6. It was shown that the unit cell is indeed face-centered cubic and that an alternate solution,[4] a primitive cubic $CsPF_6$ structure, can be ruled out for both compounds. The number of observed peaks is rather small, but the respective intensities due to the substitution of hydrogen by deuterium (scattering lengths $b_H = -0.374$ and $b_D = 0.667$) are very different (Table II). The rapid vanishing of intensities at large diffraction angles and the presence of a bump in the background level implying a short distance order are characteristic of plastic phases with ions in motion. The only models that could be tested to describe such a motion have been tried successively.

The first one is a disordered model with statistical occupancy factors for fluorine atoms and hydrogen atoms in the *Fm*3 symmetry group. This corresponds to four equivalent positions of the octahedra around the fourfold axes, and to eight positions for the OH_3^+ ion. With use of the intensities observed for OH_3AsF_6, the solution refines to $R = 0.047$ but is not considered acceptable because the resulting distances As–F = 1.58 Å and O–H = 0.82 Å are too short when compared to As–F = 1.719 (3) Å in $KAsF_6$[20] and O–H = 1.011 (8) Å in OH_3^+p-$CH_3C_6H_4SO_3^-$.[21]

The second one is a rotating model that places As at the 0, 0, 0 position connected to fluorines by a complex term

$$b_{As} + 6b_F[(\sin x)/x] \qquad x = 4\pi r_F(\sin\theta)/\lambda$$

and O at the $^1/_2$, $^1/_2$, $^1/_2$ position connected to H atoms by

$$b_O + 3b_H[(\sin x)/x] \qquad x = 4\pi r_H(\sin\theta)/\lambda$$

where b_{As}, b_F, b_O, and b_H are the scattering lengths of As, F, O, and H, respectively. The As–F distance, r_F, and the O–H distance, r_H, are the only unknowns with the scale factor of the structure.[22] The best results ($R = 0.059$) are obtained with the combination As–F = 1.59 Å and O–H = 0.81 Å, not so different indeed from the first model.

For OD_3AsF_6, the second model gives more plausible distances, As–F = 1.65 Å and O–D = 1.01 Å with $R = 0.054$, if the intensity of the 200 reflections is arbitrarily lowered by 20%, with the excessive intensity being assumed to be due to preferential orientation.

On the basis of the short distances found for OH_3AsF_6, we can consider that the real structure is probably not properly accounted for by either one of the models, due to the motion of the ions, which is not correctly simulated as for other plastic phases.

OH_3SbF_6. On the basis of the DSC data (see above), the transition from an ordered to a disordered phase occurs at 88 ± 12 °C. The existence of an ordered phase at room temperature for OH_3SbF_6 and its deuterated analogues was confirmed by the diffraction studies. The X-ray powder diffraction pattern, which originally had been read backwards due to very intense back-reflections and indexed incorrectly as tetragonal,[4] is listed in Table III. By analogy with a large class of other MF_6^- compounds such as O_2PtF_6[23] and O_2SbF_6,[24] the OH_3SbF_6 pattern can be indexed for a cubic unit cell with $a = 10.143$ (3) Å (CEN) data or 10.090 Å (Rocketdyne data). The cell dimensions were confirmed by a single-crystal X-ray study at Leicester (see below) that resulted in $a = 10.130$ (8) Å. Although all of the observed X-ray reflections obey the conditions ($h + k + l = 2n$ and $0kl$ where $k, l = 2n$) for space group *Ia*3, the neutron diffraction data (see below) suggest a lower symmetry subgroup such as $I2_13$. In the following paragraphs the results obtained for the ordered cubic, room-temperature phase of OH_3SbF_6 are discussed in more detail.

Table III. Room-Temperature X-ray Powder Data for OH_3SbF_6[a]

d_{obsd}, Å	d_{calcd}, Å	intens	h	k	l
5.04	5.04	vs	2	0	0
3.56	3.57	vs	2	2	0
2.909	2.912	mw	2	2	2
2.691	2.696	w	3	2	1
2.519	2.522	mw	4	0	0
2.374	2.378	w	4	1	1
2.254	2.256	m	4	2	0
2.149	2.151	mw	3	3	2
2.060	2.059	s	4	2	2
1.979	1.978	w	4	3	1
1.784	1.783	ms	4	4	0
1.682	1.681	ms	6	0	0, 4 4 2
1.637	1.636	vw	5	3	2
1.596	1.595	ms	6	2	0
1.519	1.521	ms	6	2	2
1.456	1.456	w	4	4	4
1.398	1.399	ms	6	4	0
1.372	1.373	vw	6	3	3
1.349	1.348	ms	6	4	2
1.282	1.281	vw	7	3	2, 6 5 1
1.262	1.261	vw	8	0	0
1.225	1.223	m	8	2	0, 6 4 4
1.189	1.189	m	8	2	2, 6 6 0
1.159	1.157	w	6	6	2
1.129	1.128	m	8	4	0
1.103	1.101	m	8	4	2

[a] Cubic, $a = 10.09$ Å, $V = 1027.2$ Å^3, $Z = 8$, $\rho_{calcd} = 3.296$ g cm^{-3}, Cu Kα radiation, Ni filter.

Single-Crystal X-ray Study. The OH_3SbF_6 single crystal had the approximate dimensions 0.46 × 0.35 × 0.22 mm and was sealed in a Pyrex capillary. Preliminary cell dimensions were obtained from Weissenberg and precession photographs. The final value for the unit cell parameter was determined from the optimized counterangles for zero-layer reflections on a Stoe Weissenberg diffractometer. The data were collected for layers $0kl$ to $6kl$ of the aligned pseudotetragonal cell, using the Stoe Stadi-2 diffractometer, in the four quadrants $h,\pm k,\pm l$ and an ω-scan technique with graphite-monochromated Mo Kα radiation. The intensities of reflections with $0.086 \leq (\sin\theta)/\lambda \leq 0.702$ Å^{-1} were collected and a total of 719 reflections obtained with $I/\sigma(I) \geq 3$. Check reflections were monitored during the data collection of each layer, and no deterioration of the crystal was indicated. Lorentz and polarization corrections were made to the data set.

The program system SHELX[25] was used to solve the structure. Neutral scattering factors were used with anomalous dispersion coefficients. Three cycles of least-squares refinement with antimony at ($^1/_2$, $^1/_2$, $^1/_2$) in the space group *Ia*3 gave an R factor of 0.27. The Fourier difference map located a 9 e Å^{-3} peak, assumed to be oxygen, on the position ($^1/_4$, $^1/_4$, $^1/_4$), with two sets of possible fluorine octahedra each at 1.90 Å from Sb. Three cyles of refinement with the oxygen atom included reduced the R factor to 0.22. The inclusion of either of the sets of F atoms about Sb, with all atoms refining isotropically, resulted in a reduced R factor of 0.13; however, the refinment cycles moved the F atoms to >2.0 Å from Sb. The inclusion of fluorine atoms also resulted in a more complex difference Fourier map, with several peaks ≈3 e Å^{-3} remaining. The alternate fluorine atom positions indicated were refined in partially occupied sites, initially adjusting the site occupation factors and then their temperature factors. The resultant R factor of 0.12 was not significantly less than with either ordered structure; one of the partial fluorine atoms refined to a position

(20) Gafner, G.; Kruger, G. J. *Acta Crystallogr., Sect. B: Struct. Crystallogr. Cryst. Chem.* **1974**, *B30*, 250.
(21) Lundgren, J. O.; Williams, J. M. *J. Chem. Phys.* **1973**, *58*, 788.
(22) APL program written by G. Langlet.
(23) Ibers, J. A.; Hamilton, W. C. *J. Chem. Phys.* **1966**, *44*, 1748.
(24) McKee, D. E.; Bartlett, N. *Inorg. Chem.* **1973**, *12*, 2738.
(25) Sheldrick, G. M. "SHELX, A Program for Structure Determination"; University of Cambridge: Cambridge, England, 1976.

Table IV. Final Atomic Positional and Thermal Parameters (with Esd's in Parentheses) for OH_3SbF_6 from X-ray Data

atom	x	y	z	U_{11}	U_{22}	U_{33}
Sb	0.5	0.5	0.5	0.0205 (18)		
O	0.25	0.25	0.25	0.043 (17)		
F	0.4334 (33)	0.6444 (34)	0.6021 (22)	0.059 (20)	0.158 (35)	0.003 (12)
H	not located					

	dist, Å		angle, deg
Sb-F	1.891 (19)	F-Sb-F	180
Sb-O	4.386	F-Sb-F	89.5 (1.0)
O-F	2.63	F-Sb-F	90.5 (1.0)
F-F	2.68/2.71		

Table V. X-ray and Neutron Powder Patterns of OD_3SbF_6 at Room Temperature

hkl	X-ray	neutron	hkl	X-ray	neutron
200	100	6	710/550/543	···	1
211	···	2	640	11	8
220	70	100	721/633/552	1	8
222	13	8	642	21	9
321	3	30	730	···	3
400	7	2	732/651	2	18
411/330	6	13	800	4	···
420	17	17	811/741/554	···	7
332	4	22	820/644	11	9
422	36	18	653	···	3
431/510	3	13	822/660	10	2
440	19	14	831/750/743	···	4
433/530	21	3	662	4	···
442/600	2	7	752	···	3
611/532	2	9	840	6	2
620	21	3			
541	1	14			
622	12	5			
631	···	2			
444	4	4			

2.2 Å from Sb, and further possible fluorine sites appeared in the Fourier map. Refinement of various models with either ordered fluorine atoms or disordered atoms constrained to be 1.86 (3) Å from antimony did not improve the R factor or the residual Fourier map. Accordingly, the F atom parameters given in Table IV represent an ordered solution in $Ia3$; the actual F atom chosen was that which remained at the expected distance from antimony during the various trial refinements. This represents an incomplete solution, as there are residual peaks at Sb–F distances in the final Fourier difference map. This is reflected in the structure factors, where agreement between $|F_o|$ and $|F_c|$ is good for even, even, even reflections with dominant contributions by the antimony and oxygen atoms but poor for odd, odd, even reflections, which are dependent only upon the fluorine (and hydrogen) atom parameters. Final residual indices for 155 unique reflections are R = 0.119 and R_w = 0.131.

Neutron Powder Diffraction Study. For OD_3SbF_6, 46 reflections were observed (see Figure 1) out of which 4 could not be indexed on the basis of the cubic cell and are attributed to an unidentified impurity (mainly lines at 3.269, 2.235, and 2.225 Å). The list of observed reflections is given in Table V in comparison with X-ray data. The cell parameter is 10.116 (6) Å.

The Rietveld program for profile refinement[26] was used to solve the structure. The first refinement was attempted in the $Ia3$ space group starting from the X-ray values for Sb, O, and F and adding approximate values for D, with the OD_3^+ ion

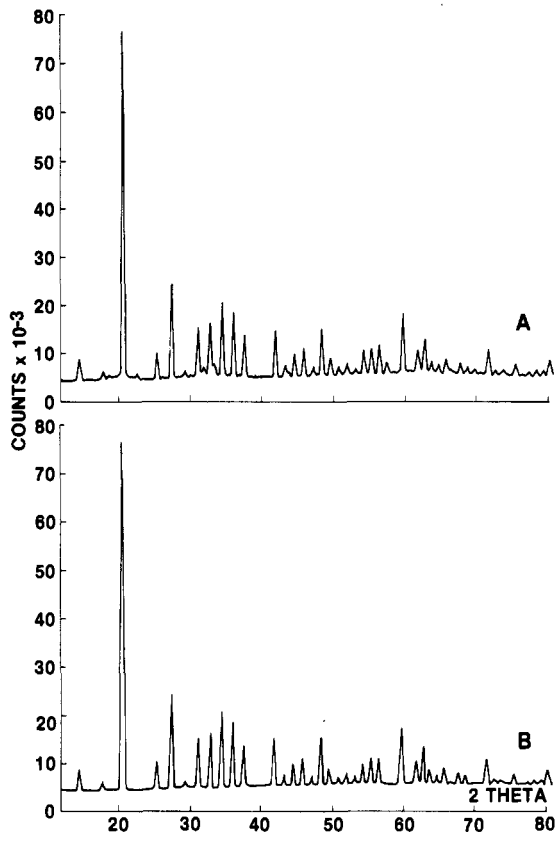

Figure 1. Neutron powder diffraction diagram of OD_3SbF_6 at ambient temperature; traces A and B, observed and calculated profiles, respectively.

being disordered on two equivalent positions (occupancy factor $^1/_2$ of general positions x, y, z). The system refined to R = 0.135 with the following parameters:

atom	x	y	z	B, Å²
Sb	0.5	0.5	0.5	0.94 (25)
O	0.25	0.25	0.25	4.87 (41)
F	0.441 (6)	0.604 (6)	0.641 (7)	2.88 (13)
D	0.300 (1)	0.317 (1)	0.204 (1)	2.98 (27)

The y and z coordinates of the fluorine atom have been permuted, probably due to the choice of the coordinates of deuterium. The atomic distances and angles are then

	dist, Å		dist, Å		angle, deg
Sb-F	1.87	O--D	0.96	DOD	108
O-F	2.67	D-D	1.56		

which compare relatively well with the X-ray values of Table IV. At this stage, our attention was drawn to the presence of a weak but well-isolated line at an angle θ high enough not be be attributed to the impurity. This line corresponded to a 730 reflection, a forbidden reflection in the space group $Ia3$ ($hk0$; $h, k = 2n$). In view of a similar observation for the cubic phase of $KSbF_6$ (II) (in this case the 310 reflection),[27] the trouble with locating the fluorine atoms by difference X-ray syntheses, and mainly the incompatibility of the group $Ia3$ with the observed Raman and IR spectra (see below), we considered the possibility of an ordered structure in a subgroup of the $Ia3$ space group, first the noncentrosymmetric $I2_13$ space group (No. 199).

Since the symmetry center does not exist anymore, the local symmetry of the Sb and O atoms is then only a threefold axis. The structure has to be described with two sets of fluorine atoms F_1 and F_2, and the oxonium ion is ordered with a full

(26) Rietveld, H. M. *J. Appl. Crystallogr.* **1969**, *2*, 65.

(27) Heyns, A. M.; Pistorius, C. W. F. T. *Spectrochim. Acta, Part A* **1976**, *32A*, 535.

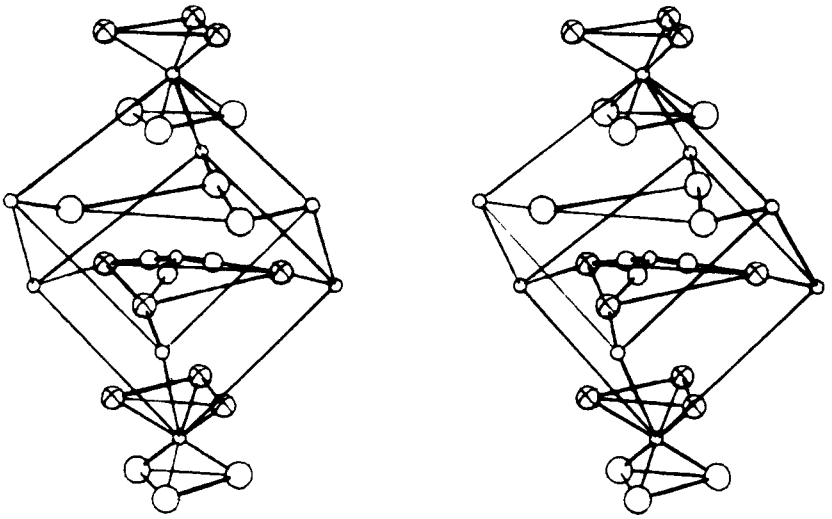

Figure 2. ORTEP stereoview of the structure of OD_3SbF_6. The bridging F_2 atoms are differentiated from the nonbridging F_1 atoms by smaller circles marked by traces.

occupation of deuterium atoms on the general positions. The Sb and O atoms are also allowed to move along the threefold axes from their ideal positions (0, 0, 0; $^1/_2$, $^1/_2$, $^1/_2$).

This hypothesis was tested and led to a better R factor (0.106) with the following parameters:

atom	x	y	z	B, Å^2
Sb	−0.012 (1)	−0.012 (1)	−0.012 (1)	0.13 (0.38)
O	0.238 (3)	0.238 (3)	0.238 (3)	3.50 (0.75)
F_1	0.044 (1)	−0.118 (1)	−0.143 (2)	1.26 (0.42)
F_2	−0.75 (2)	0.091 (1)	0.137 (2)	1.89 (0.45)
D	0.199 (2)	0.184 (1)	0.299 (1)	3.40 (0.30)

Figure 1 gives the resulting profile of observed and calculated neutron diffraction diagrams and shows satisfactory agreement.

The Sb and O atoms are displaced from their ideal positions by 0.21 Å, and the environment of the Sb atom has 3 F_1 atoms at 1.80 Å and 3 F_2 atoms at 1.94 Å, which seems to be compatible with the Raman and IR spectra.

The F_2 atoms are closer to the oxygen atom of the oxonium group than the F_1 atoms with F_2–O = 2.60 Å and F_1–O = 2.79 Å. The F_2–O distance is within the correct range for a strong OD···F hydrogen bridge bond (2.51–2.56 Å in OH_3TiF_5[9] and 2.58–2.61 Å in OH_3BF_4[10]).

The deuterium atoms are located at 0.91 Å from the oxygen atom (with a D–D distance of 1.54 Å and a DOD angle of 116°) on the line O–F_2 (OD + DF_2 = 0.91 + 1.69 = 2.60 Å). This confirms, in the precision of our results, the quasi-linearity of the O–D···F bond in this compound. The geometry of the OD_3^+ cation itself is a flat pyramid with C_3 symmetry. The oxygen atom lies 0.18 Å out of the plane of the three deuterium atoms.

Figure 2 illustrates the environment around the oxonium ion, with the F_2 atoms being differentiated from the F_1 atoms by traces of the ellipses. The two SbF_6^- octahedra fully represented are approximately located at 0, 0, 0 and $^1/_2$, $^1/_2$, $^1/_2$ along the [1, 1, 1] direction and bring the environment to an icosahedron. The distinction between F_1 and F_2 implies a small displacement of the fluorine atoms from their average positions obtained in the $Ia3$ space group (F–F_1 or F–F_2 distances are about 0.20 Å), but the angular distortion of the octahedron is small, one side being flattened and the other one being elongated. To obtain a refinement in the $I2_13$ symmetry group, we had to allow the existence of antiphase domains without local symmetry centers, but which are images of each other.

The interesting point of this structure is the existence of an ordered solution for all atoms with a scheme of hydrogen bonding that prevents at room temperature the existence of a plastic phase. Such a phase may however exist at higher temperatures and explains the phase changes observed before the decomposition point. To obtain more information on the motions of the ions in the different phases, additional experimental data such as second moment and relaxation time NMR measurements are required.

As far as the exact geometry of the OD_3^+ cation is concerned, it must be pointed out that the precision of the results obtained from the powder diffraction data is not very high and that the final values depend on the starting points used for the different refinements. Thus, the O–D distance was found to vary from 0.91 to 1.05 Å, with the ODO angle varying from 116 to 92°. The correct values certainly lie between these extreme values. This is also reflected by the higher thermal parameters found for the deuterium and oxygen positions (see above), indicating high thermal motion of the OD_3^+ cation itself. For the O–H bond length in OH_3^+, a lower limit of 0.97 Å appears more realistic for the following reasons: The bond length in free OH_2 is already 0.96 Å, and both the hydrogen–fluorine bridging and the increased $O^{\delta-}$–$H^{\delta+}$ polarity of the O–H bond in OH_3SbF_6 are expected to increase the O–H bond length. This bond weakening in OH_3^+ when compared to free OH_2 is also supported by the force constant calculations given below. The most likely range of the O–H bond length in these OH_3MF_6 salts is therefore 0.98–1.05 Å, which is in excellent agreement with the values of 1.013 (8), 1.020 (3), and 0.994 (5) Å previously found for $OH_3^+CH_3C_6H_4SO_3^-$,[21] $OD_3^+CH_3C_6H_4SO_3^-$,[28] and $OH_3^+CF_3SO_3^-$,[29] respectively, by neutron diffraction and values of 1.01–1.04 Å for $OH_3^+NO_3^-$ and $OH_3^+ClO_4^-$, derived from wide-line NMR measurements.[30]

The value of 1.19 Å, previously reported[9] for the O–H bond length in $OH_3^+BF_4^-$, is based on X-ray data and therefore is deemed unreliable. It should be pointed out that the OH···F distances in $OH_3^+BF_4^-$ and $OD_3^+AsF_6^-$ are practically identical (2.60 Å). This suggests that r_{O-H} and r_{O-D} in these two compounds should also be similar.

The neutron model was tested against the X-ray data for OH_3SbF_6, but there was no improvement in the refinement or the appearance of the Fourier difference map.

Vibrational Spectra. Although many papers have been published on the vibrational spectra and force field of the

(28) Finholt, J. E.; Williams, J. M. *J. Chem. Phys.* **1973**, *59*, 5114.
(29) Lundgren, J. O.; Tellgren, R.; Olovsson, I. *Acta Crystallogr., Sect. B: Struct. Crystallogr. Cryst. Chem.* **1978**, *B34*, 2945.
(30) Herzog-Cance, M. H.; Potier, J.; Potier, A. *Adv. Mol. Relaxation Interact. Processes* **1979**, *14*, 245.

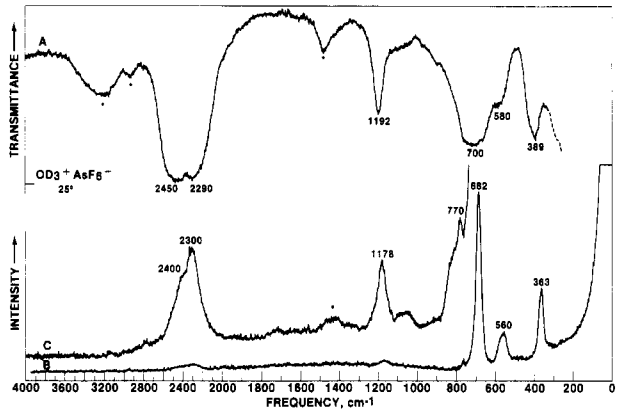

Figure 3. Vibrational spectra of solid OD_3AsF_6 at room temperature: trace A, infrared spectrum of the solid pressed between AgCl disks (broken line indicates absorption due to the window material; bands marked by an asterisk are due to OD_2H^+ mainly formed during sample handling); traces B and C, Raman spectra recorded at two different sensitivities with a spectral slit width of 3 and 8 cm^{-1}, respectively.

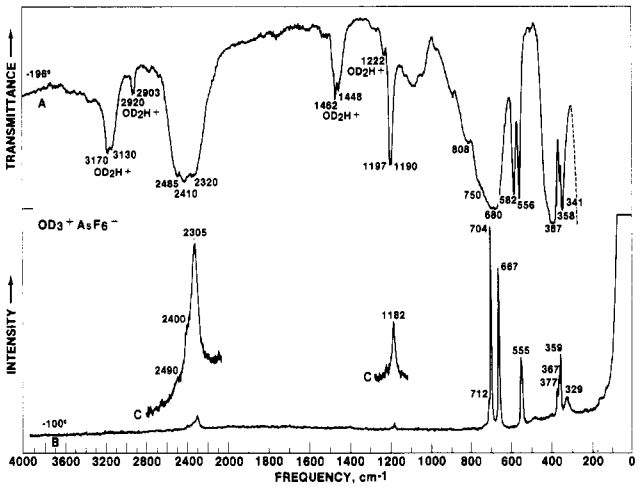

Figure 4. Vibrational spectra of solid OD_3AsF_6 at low temperature: trace A, infrared spectrum of the solid pressed between AgCl disks and recorded at −196 °C; traces B and C, Raman spectra recorded at −100 °C at two different sensitivities.

oxonium ion,[4-9,31-45] many discrepancies exist among these data. Frequently, the infrared bands observed for the stretching modes are very broad and overlap and are complicated by Fermi resonance with combination bands. Also, the smooth transition from highly ionic OH_3^+ salts to proton-transfer complexes and the interpretation of some of the more weakly ionized proton-transfer complexes in terms of discrete OH_3^+ salts may have significantly contributed to the

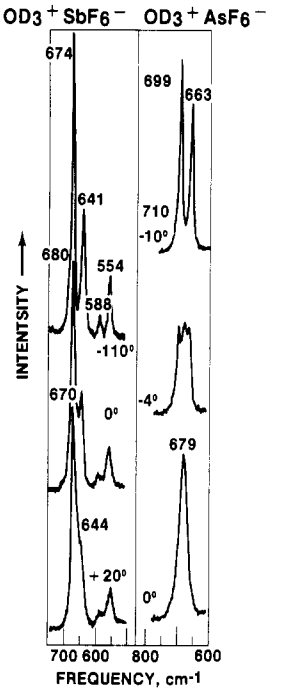

Figure 5. Raman spectra of OD_3SbF_6 and OD_3AsF_6 at different temperatures contrasting the slow gradual temperature induced line broadening for the ordered OD_3SbF_6 phase against the abrupt change within a narrow temperature range for OD_3AsF_6 caused by the transition from an ordered to a plastic phase.

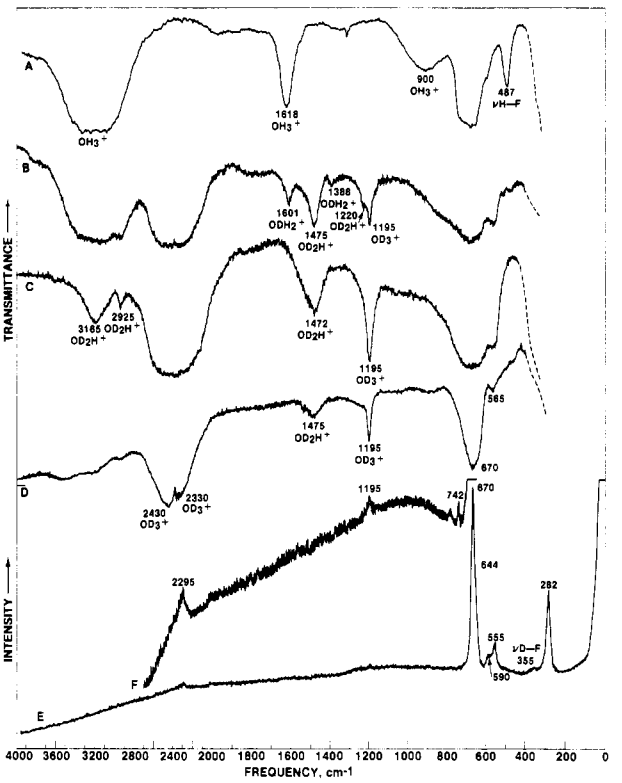

Figure 6. Vibrational spectra of solid OD_3SbF_6, OH_3SbF_6, and partially deuterated OH_3SbF_6 at room temperature: trace A, IR spectrum of OH_3SbF_6; trace B, IR spectrum of partially deuterated OH_3SbF_6 containing about equimolar amounts of OD_3SbF_6 and OD_2HSbF_6 and smaller amounts of ODH_2SbF_6; trace C, IR spectrum of OD_3SbF_6 containing a significant amount of OD_2HSbF_6 formed during sample handling; trace D, IR spectrum of OD_3SbF_6 containing only a small amount of OD_2HSbF_6; traces E and F, Raman spectra of OD_3SbF_6 recorded at two different sensitivities.

(31) Bethell, D. E.; Sheppard, N. *J. Chem. Phys.* **1953**, *21*, 1421.
(32) Ferriso, C. C.; Hornig, D. F. *J. Am. Chem. Soc.* **1953**, *75*, 4113; *J. Chem. Phys.* **1955**, *23*, 1464.
(33) Fournier, M.; Roziere, J. *C. R. Hebd. Seances Acad. Sci., Ser. C* **1970**, *270*, 729.
(34) Fournier, M.; Mascherpa, G.; Rousselet, D.; Potier, J. *C. R. Hebd. Seances Acad. Sci., Ser. C* **1969**, *269*, 279.
(35) Millen, D. J.; Vaal, E. G. *J. Chem. Soc.* **1956**, 2913.
(36) Taylor, R. C.; Videale, G. L. *J. Am. Chem. Soc.* **1956**, *78*, 5999.
(37) Mullhaupt, J. T.; Hornig, D. F. *J. Chem. Phys.* **1956**, *24*, 169.
(38) Basile, L. J.; La Bonville, P.; Ferraro, J. R.; Williams, J. M. *J. Chem. Phys.* **1974**, *60*, 1981.
(39) Ferraro, J. R.; Williams, J. M.; La Bonville, P. *Appl. Spectrosc.* **1974**, *28*, 379.
(40) Huong, P. V.; Desbat, B. *J. Raman Spectrosc.* **1974**, *2*, 373.
(41) Gilbert, A. S.; Sheppard, N. *J. Chem. Soc., Faraday Trans. 2* **1973**, *69*, 1628.
(42) Savoie, R.; Giguere, P. A. *J. Chem. Phys.* **1964**, *41*, 2698.
(43) Schneider, M.; Giguere, P. A. *C. R. Hebd. Seances Acad. Sci., Ser. C* **1968**, *267*, 551.
(44) Desbat, B.; Huong, P. V. *Spectrochim. Acta, Part A* **1975**, *31A*, 1109.
(45) Giguere, P. A.; Turrell, S. *J. Am. Chem. Soc.* **1980**, *102*, 5473; *Can. J. Chem.* **1976**, *54*, 3477.

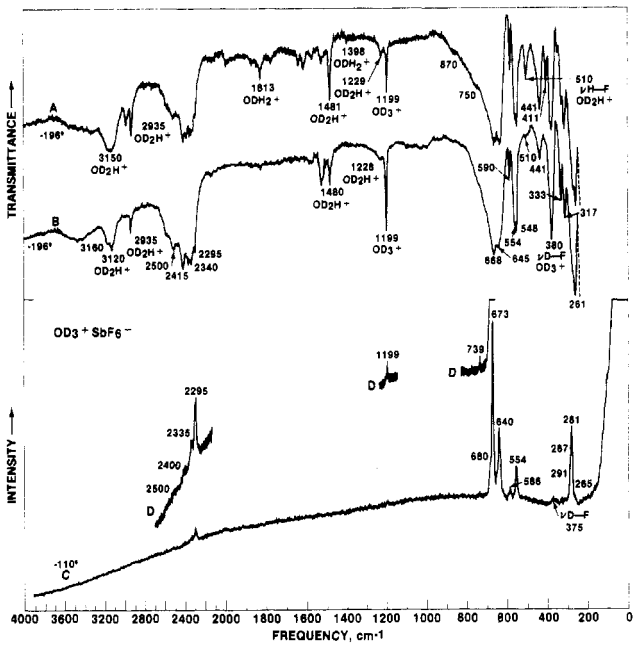

Figure 7. Vibrational spectra of solid OD_3SbF_6 and partially deuterated OH_3SbF_6 at low temperature: traces A and B, infrared spectra of partially deuterated OH_3SbF_6 and of OD_3SbF_6, respectively, between AgBr windows; traces C and D, Raman spectra recorded at two different sensitivities.

general confusion. As a consequence, there is still considerable ambiguity[4] whether the antisymmetric or the symmetric OH_3^+ stretching mode has the higher frequency. Furthermore, the symmetric OH_3^+ deformation mode is generally very difficult to locate due to the great line width of the band.[46] Although vibrational spectra have previously been reported for OD_3^+,[32,34,38] they have been of little help to strengthen the vibrational assignments for the oxonium cation. Consequently, it was interesting to record the vibrational spectra of deuterated and partially deuterated OH_3^+ in salts containing well-defined discrete oxonium cations. We hoped to verify the above described phase changes and to compare the experimentally observed spectra with the results from recent theoretical calculations[47-49] and with those of the isoelectronic ammonia analogues.[50-54]

The observed infrared and Raman spectra and the more important frequencies are given in Figures 3–7 and Table VI.

Room-Temperature Spectra of OD_3AsF_6. Figure 3 shows the room-temperature spectra of solid OD_3AsF_6. As can be seen, the bands are broad and show no splittings or asymmetry as expected for ions undergoing rapid motion in a plastic phase.[4,17,19] On the basis of their relative infrared and Raman intensities, the band at about 2450 cm^{-1} can be assigned with confidence to the antisymmetric OD_3^+ stretching mode $\nu_3(E)$ and the band at about 2300 cm^{-1} to the symmetric OD_3^+ stretching mode $\nu_1(A_1)$. This assignment of $\nu_3 > \nu_1$ is further supported by all the other spectra recorded in this study (see below). Also, their frequency separation of about 150 cm^{-1} is very similar to that of 144 cm^{-1} found for isoelectronic ND_3.[50] Furthermore, a recent ab initio calculation for OD_3^+ also arrived (after applying the suggested −12.3% correction to all frequencies) at ν_3 being 165 cm^{-1} higher than ν_1 (see Table VII).[49] This finding that in a strongly hydrogen-bridged oxonium salt ν_3 is higher than ν_1 disagrees with the previous suggestion that the order of the OH_3^+ stretching frequencies should invert when r_{X-Y} in X–H···Y becomes shorter than the van der Waals radius sum.[38]

The assignment of the 1192-cm^{-1} infrared and the 1178-cm^{-1} Raman band to the antisymmetric OD_3^+ deformation $\nu_4(E)$ is straightforward and again is in excellent agreement with the frequency values of 1191 and 1161 cm^{-1}, found for isoelectronic ND_3[50] and calculated for OD_3^+ by ab initio methods,[49] respectively (see Table VII).

The assignment of the last yet unassigned fundamental of OD_3^+, the symmetric deformation mode $\nu_2(A_1)$, is more difficult. On the basis of an analogy with ND_3, this mode should occur at about 750 cm^{-1}, and indeed the Raman spectrum of OD_3AsF_6 exhibits a band at 770 cm^{-1} of about the right intensity. The failure to observe a well-defined infrared counterpart could possibly be due to its great line width. The ab initio calculations for $\nu_2(A_1)$ of OD_3^+ predict an intense infrared band at 549 cm^{-1}. Indeed the infrared spectrum of OD_3AsF_6 (trace A, Figure 3) shows a medium–strong band at 580 cm^{-1}. However, we prefer to assign this band to $\nu_2(E_g)$ of AsF_6^- for the following reasons: This mode frequently becomes infrared active in many AsF_6^- salts. Furthermore, it has also been observed in OH_3AsF_6;[4] if it were due to OD_3^+, it would have been shifted in OH_3AsF_6 to a significantly higher frequency. This assignment to ν_2 of AsF_6^- is also supported by the low-temperature infrared spectra of OH_3AsF_6 and OD_3AsF_6 (Figure 4), both of which show two sharp bands of almost identical intensities and frequencies at about 580 and 560 cm^{-1}.

The remaining bands due to AsF_6^- in OD_3AsF_6 are in excellent agreement with those previously observed for OH_3AsF_6 and can be assigned accordingly.[4] IR: $\nu_3(F_{1u})$, 700; $\nu_4(F_{1u})$, 389 cm^{-1}. Raman: $\nu_1(A_{1g})$, 682; $\nu_2(E_g)$, 560; $\nu_5(F_{2g})$, 363 cm^{-1}. Several weak bands in the spectrum of OD_3AsF_6 are marked by an asterisk. These are due to a small amount of OD_2H^+ and will be discussed below.

Low-Temperature Spectra of OD_3AsF_6. Figure 4 shows the low-temperature spectra of OD_3AsF_6. The most prominent changes from the room-temperature spectra are the pronounced sharpening of all bands accompanied by splittings. As discussed above, these changes are caused by freezing of the ion motions. The change from a plastic phase to an ordered one, occurring on the basis of DSC measurements in the −7 to +2 °C temperature range, was confirmed by Raman spectroscopy. As can be seen from Figure 5, the freezing out of the ion motion occurs indeed within the very narrow temperature range.

Compared to the room-temperature spectra, the low-temperature spectra do not provide much additional information on the fundamental vibrations of OD_3^+. The $\nu_1(A_1)$ fundamental is shown to occur at a lower frequency than $\nu_3(E)$, and $\nu_4(E)$ shows a splitting into two components in the infrared spectrum. The $\nu_2(A_1)$ deformation mode is again difficult to locate but clearly cannot be attributed to the 582-cm^{-1} infrared band for the above given reasons.

From the AsF_6^- part of the spectra some conclusions concerning the possible site symmetry of AsF_6^- might be reached. All degeneracies appear to be lifted for the fundamentals, and the bands are not mutually exclusive. This eliminates all centrosymmetric space groups and site symmetries such as O_h, T_h, or C_{3i}. The highest possible site symmetry appears to be

(46) Giguere, P. A.; Guillot, J. G. *J. Phys. Chem.* **1982**, *86*, 3231.
(47) Allavena, M.; Le Clec'h, E. *J. Mol. Struct.* **1974**, *22*, 265.
(48) Bunker, P. R.; Kraemer, W. P.; Spirko, V. *J. Mol. Spectrosc.* **1983**, *101*, 180.
(49) Colvin, M. E.; Raine, G. P.; Schaefer, H. F.; Dupuis, M. *J. Chem. Phys.* **1983**, *79*, 1551.
(50) Shimanouchi, T. *Natl. Stand. Ref. Data Ser. (U.S., Natl. Bur. Stand.)* **1972**, *39*, 15.
(51) Whitmer, J. C. *J. Chem. Phys.* **1972**, *56*, 1050.
(52) Wolff, H.; Rollar, H. G.; Wolff, E. *J. Chem. Phys.* **1971**, *55*, 1373.
(53) Reding, F. P.; Hornig, D. F. *J. Chem. Phys.* **1951**, *19*, 594; **1955**, *23*, 1053.
(54) Thornton, C.; Khatkale, M. S.; Devlin, J. P. *J. Chem. Phys.* **1981**, *75*, 5609.

Table VI. Vibrational Spectra of OD_3AsF_6, OD_3SbF_6, and Their Partially Deuterated Analogues

obsd freq, cm^{-1}, and rel intens[a] for OD_3AsF_6[c]				assgnt (point group)[b]			obsd freq, cm^{-1}, and rel intens[a]					assgnt (point group)[b]			
25 °C		−196 °C	−100 °C				OD_3SbF_6[c] 25 °C		−196 °C	$OD_nH_{3-n}SbF_6$ −110 °C	25 °C				
IR	RA	IR	RA	OD_3^+ (C_{3v})	OD_2H^+ (C_s)	AsF_6^- (O_h)	IR	RA	IR	RA	IR	−196 °C	OD_3^+ (C_{3v})	OD_2H^+ (C_s)	ODH_2^+ (C_s)	SbF_6^- (O_h)
3170 mw, br		3170, 3120 m			ν(OH)(A′)		3165 mw, br		3160 m, 3120 m		3400–3000 vs, br	3150 m		ν(OH)(A′)	$\nu_{as}(OH_2)$-(A″), $\nu_s(OH_2)$-(A′)	
2910 vw, br		2920, 2903 w			$2\delta_{as}$(A′)		2925		2935 mw, 2575 sh		2930 m	2980 w, 2935 mw		$2\delta_{as}$(A′)		
		2485 s	2490 sh	ν_{as}(E), $2\delta_{as}(A_1)$	$\nu_{as}(OD_2)$-(A″), $\nu_s(OD_2)$-(A′)				2500 m, 2415 s	2500 sh, 2400 sh	2400 vs, br	2510 m, 2410 s	ν_{as}(E), $2\delta_{as}(A_1)$	$\nu_{as}(OD_2)$-(A″), $\nu_s(OD_2)$-(A′)		
2450 vs, br	2400 sh	2410 vs	2400 sh				2430 vs, br									
2290 s, br	2300 (0.3)	2320 s	2305 (0.6)	$\nu_s(A_1)$			2330 s, br		2340 s	2335 (0+)	2320 vs, br	2340 m		ν(OD)(A′)		
1471 mw	1440 (0+)	1462, 1448 m			δ_{as}(A′)			2295 (0.2)	2295 w	2295 (0.6)		2295 w	$\nu_s(A_1)$			
		1222 vw			δ_{as}(A″)		1601 m		1523 mw		1601 m	1613 mw, 1525 w		δ_{as}(A″)		
1192 ms	1178 (0.3)	1197, 1190 ms	1182 (0.3)	δ_{as}(E)			1475 mw	1480 mw		1475 ms	1481 ms			δ_{as}(A′)		
		1030 m								1388 w	1398 w			δ_{as}(A′)		
		882 vw							1228 w		1220 w	1229 mw		δ_{as}(A″)		
	810 sh	808 m					1195 mw	1199 (0+)	1199 s		1195 ms	1199 ms	δ_{as}(E)			
	770 (0.2)	750 sh	712 sh	$\delta_s(A_1)$							900–800 sh, br	870 sh		δ_s(A′)		
700 vs, br		680 vs, br	704 (10)			$\nu_{as}(F_{1u})$		742 (0+)		680 sh		750 sh	$\delta_s(A_1)$			
	682 (10)		667 (7.9)			$\nu_s(A_{1g})$	670 vs, br	670 (10)	668 vs	673 (10), 650 sh	680 vs, br	670 vs				$\nu_{as}(F_{1u})$, $\nu_s(A_{1g})$
580 m, br		582 s														
	560 (1.6)					$\nu_s(E_g)$		644 sh	645 s	640 (4.1)		643 vs				
		556 s	555 (3.3)					590 (0.8)	590 mw	586 (0.7)		590 mw				
		510 w			ν(F···H)		565 m, br				565 m, br					
		410 sh			ν(F···D)				554 m			564 m				$\nu_s(E_g)$
389 s		387 vs				$\delta_{as}(F_{1u})$		555 (1.5)	548 ms	554 (1.8)		558 ms				
		372 sh	377 (1.2)						510 vw			510 m		ν(F···H)		
	363 (3.6)		367 (1.9)			$\delta_s(F_{2g})$			441 m			441 ms				
		358 mw	359 (2.9)						410 sh			411 m		ν(F···D)		
		341 s		ν(F···D)				355 (0.2)	380 s, 370 sh	375 (0.3)		381 s				
		325 sh	329 (0.8)									353 w	ν(F···D)			
									333 m			334 w				
									317 m			319 m				
									290 sh	291 sh		290 sh				$\delta_{as}(F_{1u})$
								282 (4.5)	275 sh, 261 vs	287 sh, 281 (4.4), 265 sh		274 sh, 262 vs				$\delta_s(F_{2g})$

[a] Uncorrected Raman intensities. [b] Idealized point groups were assumed for the ions; this approximation is reasonable for the disordered phases but is not valid for the ordered phases in which the site symmetry of the ions is C_3 or lower. [c] The spectra of these compounds contain bands due to some OD_2H^+ resulting from a small amount of H_2O in the D_2O starting material (~0.6%) and from handling of the IR samples.

Table VII. Frequencies (cm^{-1}), Frequency Shifts on Deuteration, and Relative Infrared Intensities of OD_3^+ and OH_3^+ Compared to Those of Gaseous ND_3 and NH_3[a] and to the Results from ab Initio Calculations[b]

assgnt for point group C_{3v}	approx descrpn of mode	OD_3^+ obsd	OH_3^+ obsd	$\nu(OH_3^+)$: $\nu(OD_3^+)$	ND_3	NH_3	$\nu(NH_3)$: $\nu(ND_3)$	OD_3^+ calcd	OH_3^+ calcd	$\nu(OH_3^+)_{calcd}$: $\nu(OD_3^+)_{calcd}$
$\nu_1(A_1)$	$\nu_s(XY_3)$	2300 m	3150 m	1.37	2420	3336	1.38	2424 (0.6)	3411 (1.0)	1.41
$\nu_2(A_1)$	$\delta_s(XY_3)$	715	900 m, br	1.26	748	950	1.27	549 (6.6)	725 (13.9)	1.32
$\nu_3(E)$	$\nu_{as}(XY_3)$	2450 vs	3300 vs	1.35	2564	3444	1.34	2589 (7.0)	3516 (13.5)	1.36
$\nu_4(E)$	$\delta_{as}(XY_3)$	1182 ms	1620 ms	1.37	1191	1626	1.37	1161 (1.3)	1598 (3.2)	1.38

[a] Data from ref 50. [b] Data from ref 49 after application of the suggested −12.3% frequency correction.

Table VIII. Frequencies (cm^{-1}) and Relative Infrared Intensities of OD_2H^+ and ODH_2^+ Compared to Those of Solid ND_2H and NHD_2[a] and to the Results of ab Initio Calculations[b]

assignt for point group C_s	approx descrpn of mode for XY_2Z	OD_2H^+ calcd	OD_2H^+[c] obsd	ND_2H obsd	ODH_2^+ calcd	ODH_2^+[c] obsd	NDH_2 obsd
$\nu_1(A')$	XZ str	3484 (9.9)	3150 vs	3329 s	2532 (4.4)		2447 s
$\nu_2(A')$	sym XY_2 str	2476 (2.1)		2392 m	3450 (5.8)		3300 m
$\nu_3(A')$	asym deformn	1447 (2.7)	1481 mw	1476 mw	1344 (1.7)	1398 w	1393 w
$\nu_4(A')$	sym deformn	611 (9.0)		905 vs	671 (11.5)		992 vs
$\nu_5(A'')$	asym XY_2 str	2589 (7.2)		2501 vs	3516 (13.5)		3359 vs
$\nu_6(A'')$	asym deformn	1186 (1.2)	1229 w	1254 w	1580 (3.4)	1613 mw	1602 mw

[a] Data from ref 52. [b] Data from ref 49 after application of the suggested −12.3% frequency correction. [c] Frequency values taken from the low-temperature IR spectra of the SbF_6^- salts.

C_3, in agreement with our triply hydrogen-bonded model possessing AsF_6^- ions with three shorter and three longer As–F bonds. Since that unit cell contains more than one molecule, additional splittings are possible due to in-phase out-of-phase coupling effects within the unit cell.

The low-temperature spectra of OD_3AsF_6 show a medium–strong IR band at 341 cm^{-1} and a Raman band at 329 cm^{-1}. These bands cannot be assigned to AsF_6^- because their frequencies are too low for ν_4 and also they were not observed in the low-temperature spectra of OH_3AsF_6.[4] In OH_3AsF_6, however, two corresponding bands were observed at 467 cm^{-1} (IR) and 480 cm^{-1} (Raman).[4] Since their average frequency values, 335 and 474 cm^{-1}, respectively, are exactly in a ratio of $1:2^{1/2}$, these bands must involve the hydrogen atoms and therefore are assigned to the D···F and H···F stretching modes, respectively. As expected, these bands due to H···F stretching are not observed in the plastic-phase, room-temperature spectra due to rapid motion of the ions.

From a simple diatomic model and the average observed frequency values ($\nu_{H\cdots F}$ = 474 and $\nu_{D\cdots F}$ = 335 cm^{-1}), the corresponding force constants are f_{HF} = 0.1258 mdyn/Å and f_{DF} = 0.1204 mdyn/Å, respectively. Their averaged value (0.1231 mdyn/Å) corresponds to a hydrogen bridge bond energy of 1.77 kcal mol^{-1}, indicative of a weak hydrogen bond.

Spectra of OD_3SbF_6, OH_3SbF_6, and Partially Deuterated OH_3SbF_6. Figure 6 shows the room-temperature vibrational spectra of OD_3SbF_6, OH_3SbF_6, and partially deuterated OH_3SbF_6. Although the Raman lines due to SbF_6^- (670, 590, 555, and 282 cm^{-1} in trace E) are broadened, the 670-cm^{-1} line had a pronounced shoulder at 644 cm^{-1}, the $\nu_2(E_g)$ mode is split into its two degenerate components (see Figure 5), and the D···F stretching mode at 355 cm^{-1} (trace E of Figure 6) and H···F stretching mode at 487 cm^{-1} (trace A of Figure 6) are observed. All these features clearly indicate that OD_3SbF_6 and OH_3SbF_6 are ordered at room temperature, thus confirming the above given DSC and neutron diffraction data.

The assignments for OD_3^+ in its SbF_6^- salt can be made by complete analogy to those given above for OD_3AsF_6. The increased splitting of the 2430- and 2330-cm^{-1} bands and their relative infrared intensities[49] (trace D of Figure 6) lend further support to the $\nu_3 > \nu_1$ assignment for the oxonium salts. On cooling (see Figure 7), all the important spectral features are retained, but become more evident due to better resolution caused by the narrow line widths. Thus, the D···F stretching vibrations at 380 cm^{-1} become very prominent in the infrared spectra.

An analysis of the bands attributable to SbF_6^- (IR: 668, 645, 590, 554, 548, 285 sh, 270 sh, 261 cm^{-1}. Raman: 680 sh, 673, 650 sh, 640, 586, 554, 291 sh, 287 sh, 281, 265 sh cm^{-1}.) shows again that the site symmetry can be at best C_3. Thus, the vibrational spectra appear to be compatible with a space group such as $I2_13$, which was chosen for the above given neutron diffraction structure analysis.

Assignments for OD_2H^+ and ODH_2^+. The vibrational spectra of the OD_3^+ salts showed bands at about 3160, 2920, and 1470 cm^{-1}, marked by an asterisk in Figure 3, which could not readily be attributed to combination bands of OD_3^+. Assignment of the 1470-cm^{-1} infrared band to the antisymmetric stretching mode of HF_2^- is also unsatisfactory, because the band was also observed in the Raman spectrum, which in turn did not show the expected symmetric HF_2^- stretching mode at 600 cm^{-1}. Furthermore, $OD_3^+SbF_6^-$ should result in the formation of DF_2^- and not of HF_2^-. Consequently, we have examined the possibility of these bands being due to small amounts of incompletely deuterated oxonium ions by recording the spectra of partially deuterated OH_3SbF_6. As can be seen from trace B of Figure 6, the intensity of the band at about 3160, 2920, and 1470 cm^{-1} has increased strongly for the partially deuterated sample, and therefore these bands are assigned to the OD_2H^+ cation. The observed frequencies closely correspond to those of isoelectronic ND_2H[51-54] and the ab initio calculated OD_2H^+ values[49] (see Table VIII). Consequently the 3160- and 1470-cm^{-1} bands are assigned to the OH stretching mode and the antisymmetric (A′) OD_2H deformation mode, respectively, of OD_2H^+. The 2920-cm^{-1} band can readily be assigned to the first overtone of the 1470-cm^{-1} band being in Fermi resonance with the OH stretching mode. The antisymmetric and symmetric OD_2 stretching modes of OD_2H^+ are expected to have frequencies of about 2400 and 2300 cm^{-1},[49,51-54] respectively, and therefore are hidden underneath the intense OD_3^+ stretching modes. The antisymmetric (A″) OD_2H^+ deformation mode is expected[49,51-54] to have a frequency between 1190 and 1250 cm^{-1} and therefore can be assigned to the infrared band at 1220 cm^{-1} observed in trace B of Figure 6.

In addition to the bands attributed to OD_3^+ and OD_2H^+, the infrared spectrum of the partially deuterated OH_3SbF_6 sample (calculated product distribution (mol %): OD_3^+, 51.68;

Table IX. Symmetry and Internal Force Constants[a] of OD_3^+ Compared to Those of OH_3^+, NH_3, and ND_3[b]

	force field[c]	DFF	OD_3^+ F_{22} and $F_{44} \equiv$ min	NH_3TR	OH_3^+ F_{22} and $F_{44} \equiv$ min	NH_3-ND_3 GVFF
A_1	$F_{11} = f_r + 2f_{rr}$	6.030	6.0440	6.085	5.7783	6.4540
	$F_{22} = f_\alpha + 2f_{\alpha\alpha'}$	0.4868	0.4866	0.4997	0.4382	0.4049
	$F_{12} = f_{r\alpha} + f_{r\alpha'}$	0	0.0527	0.3244	0.0242	0.3244
E	$F_{33} = f_r - f_{rr}$	6.0595	6.1194	6.133	5.9696	6.4732
	$F_{44} = f_\alpha - f_{\alpha\alpha}$	0.6041	0.6010	0.6011	0.5934	0.6161
	$F_{34} = f_{r\alpha} + f_{r\alpha'}$	0	−0.1228	−0.1622	−0.0654	−0.1622
	f_r	6.0497	6.0943	6.117	5.9058	6.4668
	f_{rr}	−0.0098	−0.0251	−0.016	−0.0638	−0.0064
	f_α	0.5650	0.5629	0.5673	0.5417	0.5457
	$f_{\alpha\alpha}$	−0.0391	−0.0381	−0.0338	−0.0517	−0.0704
	$f_{r\alpha}$	0	0.0582	0.1622	0.0355	0.1622
	$f_{r\alpha'}$	0	−0.0646	0	−0.0299	0

[a] Stretching constants in mdyn/Å, deformation constants in mdyn Å/rad², and stretch-bend interaction constants in mdyn/rad. The following bond angles and lengths were used: OD_3^+ and OH_3^+, 110° and 1.01 Å; NH_3, 107° and 1.01 Å. The bending coordinates were weighted by unit (1-Å) distance. Frequency values: OD_3^+, $\nu_1 = 2300$, $\nu_2 = 715$, $\nu_3 = 2450$, $\nu_4 = 1182$; OH_3^+, $\nu_1 = 3150$, $\nu_2 = 900$, $\nu_3 = 3300$, $\nu_4 = 1620$ cm⁻¹. [b] Values from ref 57 with the assumption $F_{12} = -2F_{34}$. [c] The potential energy distribution for OD_3^+ showed all fundamentals to be close to or 100% characteristic, with the largest amount of mixing being observed for ν_4 in the NH_3 transfer force field of OH_3^+.

OD_2H^+, 38.16; ODH_2^+, 9.33; OH_3^+, 0.77) exhibits two bands at 1601 and 1388 cm⁻¹ (see trace B of Figure 6). These band are in excellent agreement with our expectations[49,51-54] (see Table VIII) for $\delta_{as}(A'')$ and $\delta_{as}(A')$, respectively, of ODH_2^+ and are assigned accordingly. The OD and OH_2 stretching modes of ODH_2 are again buried in the broad intense bands centered at about 2400 and 3300 cm⁻¹ and therefore cannot be located with any reliability. The symmetric deformation modes of OD_2H^+ and ODH_2^+ are probably giving rise to the strong shoulder in the 800–900 cm⁻¹ range (trace B of Figure 6) but cannot be located precisely due to their broadness.

The above assignments for OD_2H^+ and ODH_2^+ are further substantiated by the low-temperature spectra shown in Figures 4 and 7, with the decreased line widths allowing a more precise location of the individual frequencies. Most of the infrared bands observed in the 320–510 cm⁻¹ region for the low-temperature spectra of the different oxonium SbF_6^- salts are attributed to the D···F and H···F stretching modes of the hydrogen bridges.

In summary, most of the features observed for the vibrational spectra of the oxonium salts can satisfactorily be accounted for by the assumption of disordered higher temperature and ordered, hydrogen-bridged, lower temperature phases. Reasonable assignments can be made for the series OH_3^+, ODH_2^+, OD_2H^+, and OD_3^+ (see Table VI) that are in excellent agreement with those of the corresponding isoelectronic ammonia molecules[51-54] and the results of recent ab initio calculations[49] (see Tables VII and VIII). The only discrepancy between the ab initio calculations and the experimental data exists in the area of the symmetric deformation modes. This could be caused by the low barrier to inversion in OH_3^+.[49]

Force Constants. In view of our improved assignments for the oxonium cation, it was interesting to redetermine its force field. The frequencies and assignments given in Table VIII, a bond length of 1.01 Å, and a bond angle of 110° were used to calculate a valence force field of OD_3^+ by using a previously described method[4] to obtain an exact fit between calculated and observed frequencies. The results of these computations are summarized in Table IX.

Since isotopic shifts obtained by light-atom substitution such as H–D are virtually useless for the determination of a general valence force field,[55] approximating methods were used. Three different force fields were computed for OD_3^+ to demonstrate that for a vibrationally weakly coupled system such as OD_3^+ the choice of the force field has little influence on its values. Our preferred force field is that assuming F_{22} and F_{44} being a minimum. This type of force field has previously been shown[56] to be a good approximation to a general valence force field for vibrationally weakly coupled systems. As can be seen from Table IX, the force field obtained in this manner is indeed very similar to the general force field previously reported[57] for ND_3 and NH_3. The fact that the force constants of OD_3^+ deviate somewhat from those of OH_3^+ is mainly due to the broadness of the OH_3^+ vibrational bands and the associated uncertainties in their frequencies. Since the stretching frequencies of OD_3^+ are more precisely known that those of OH_3^+, the OD_3^+ force field should be the more reliable one. The fact that F_{12} in NH_3 and ND_3 is somewhat larger than the value obtained for F_{12} in our F_{22} = minimum force field is insignificant because in the published[57] NH_3 force field F_{12} was not well determined and was consequently assumed to equal $-2F_{34}$. The fact that the stretching force constant f_r in OD_3^+ is slightly lower and the deformation constant f_α in OD_3^+ is slightly higher than those in ND_3 is not unexpected. The ND_3 frequencies were those of the free molecule, whereas the OD_3^+ values are taken from the ionic solid $OD_3^+AsF_6^-$. In this solid, D–F bridging occurs (see above), thereby lowering the OD stretching and increasing the deformation frequencies. As secondary effects, the higher electronegativity of oxygen and the positive charge in OD_3^+ are expected to increase the polarity of the O–D bonds,thereby somewhat decreasing all the frequencies. These explanations can well account for the observed differences.

For the bending force constant f_α, values of 0.563 and 0.542 mdyn Å/rad² were obtained for OD_3^+ and OH_3^+, respectively. These values are in excellent agreement with the value of 0.55 mdyn Å/rad² obtained for OH_3^+ by an ab initio calculation.[47]

In summary, the results from our normal-coordinate analysis lend strong support to our analysis of the vibrational spectra. They clearly demonstrate the existence of discrete OH_3^+ ions that in character closely resemble the free NH_3 molecule, except for some secondary effects caused by hydrogen–fluorine bridging.

Conclusion. The results of this study show that OD_3AsF_6 exists at room temperature in a plastic phase, whereas OD_3SbF_6 has an ordered structure. Based on diffraction data and vibrational spectra, a structural model is proposed for the ordered phase of OD_3SbF_6. More experimental data are needed to define the exact nature of the ion motions and the associated phase changes in these salts. Many of the obser-

(55) Mohan, N.; Mueller, A.; Nakamoto, K. *Adv. Infrared Raman Spectrosc.* **1975**, *1*, 180.
(56) Sawodny, W. *J. Mol. Spectrosc.* **1969**, *30*, 56.
(57) Shimanouchi, T.; Nakagawa, I.; Hiraishi, J.; Ishii, M. *J. Mol. Spectrosc.* **1966**, *19*, 78.

vations made in this study are in poor agreement with previous reports for other oxonium salts and cast some doubt on the general validity of some of the previous conclusions. Due to their good thermal stability, oxonium salts of complex fluoro cations are well suited for further experimental studies.

Acknowledgment. The authors are indebted to Drs. C. Schack, R. Wilson, and W. Wilson of Rocketdyne, Dr. P. Meriel of CEN Saclay, and Dr. P. Aldebert of ILL Grenoble for their help with experiments. K.O.C. thanks the U.S. Army Research Office and the Office of Naval Research for financial support.

Registry No. $OH_3^+AsF_6^-$, 21501-81-5; $OD_3^+AsF_6^-$, 92186-28-2; $O_2^+AsF_6^-$, 12370-43-3; $OD_3^+SbF_6^-$, 92186-29-3; $OH_3^+SbF_6^-$, 55649-03-1; D_2O, 7789-20-0; DF, 14333-26-7; AsF_5, 7784-36-3; SbF_5, 7783-70-2; $OD_2H^+SbF_6^-$, 92186-30-6; $ODH_2^+SbF_6^-$, 92186-31-7; OD_3^+, 24847-51-6; MoF_4O, 14459-59-7; D_2, 7782-39-0.

Contribution from the School of Science, Griffith University, Nathan, Queensland 4111, Australia, and Department of Physical and Inorganic Chemistry, University of Western Australia, Nedlands, Western Australia 6009, Australia

Lewis Base Adducts of Group 1B Metal(I) Compounds. 8. High-Resolution Solid-State ^{31}P Nuclear Magnetic Resonance Spectra of Tetrameric (Triphenylphosphine)copper(I) Halide Complexes and Crystal Structure Determination of Cubane $[PPh_3CuBr]_4$

PETER F. BARRON,[1a] JEFFREY C. DYASON,[1a] LUTZ M. ENGELHARDT,[1b] PETER C. HEALY,*[1a] and ALLAN H. WHITE[1b]

Received January 6, 1984

Crystal structure analysis of the tetrameric 1:1 adduct of PPh_3 with CuBr, $[CuBrPPh_3]_4$, recrystallized from refluxing toluene, shows that it has crystallized in a "cubane" rather than the previously recorded "step" form. A residual of 0.044 was obtained for 3708 independent observed diffractometer reflections recorded at 295 K after full-matrix least-squares refinement; crystals are isomorphous with the chloride, with an orthorhombic *Pbcn* cell, a = 17.662 (5) Å, b = 20.748 (7) Å, c = 18.351 (6) Å, and Z(tetramer) = 4. The existence of the cubane form of the bromide was discovered during high-resolution solid-state ^{31}P NMR spectral studies on a series of cuprous halide–triphenylphosphine complexes.

Introduction

Modern structural studies of the tetrameric 1:1 adducts of copper(I) and silver(I) halides with triphenylphosphine have shown that while the copper(I) chloride adduct crystallizes in a "cubane" form,[2] the bromide and iodide adducts both crystallize as "step" structures.[3,4] The analogous silver(I) adducts all crystallize as cubane structures;[5-7] the iodide, however, can also be induced to crystallize in the step form.[7] The step structure is less sterically constrained than the cubane structure and is postulated to be the preferred structural form for combinations with large halide and ligand molecules.[7] However, the reported cubane structure for the adduct of copper(I) iodide with sterically demanding ligands,[8,9] the existence of step and cubane structures for the silver complexes mentioned above, and evidence that $[AsPh_3CuI]_4$ exists in both forms[10] suggest that both types of structures can accommodate wide variations in electronic and steric properties of the constituent molecules and that it may be possible to crystallize both forms for some adducts with only small changes in experimental conditions.

As part of a program investigating the high-resolution solid-state NMR spectra of complexes of univalent group 1B metals, we recorded the ^{31}P spectra of $[PPh_3CuCl]_4$, $[PPh_3CuBr]_4$, and $[PPh_3CuI]_4$, prepared according to literature methods.[11] Similarities between the spectra of the chloride and bromide complexes suggested that they could be isostructural, giving rise to the possibility that one of them could be induced to crystallize in both cubane and step forms. Subsequent structural determination of the bromide complex showed that it, in fact, had crystallized in the cubane form. In this report we describe the ^{31}P solid-state NMR results for these compounds and the determination of the crystal and molecular structure of cubane $[PPh_3CuBr]_4$.

Experimental Section

^{31}P NMR spectra were obtained on a Bruker CXP-300 spectrometer at 121.47 MHz using ^1H–^{31}P cross polarization with rf fields of 8 and 20 G for ^1H and ^{31}P, respectively. Single contacts of 1 ms were used with spin temperature alternation and recycle times of between 10 and 50 s, depending on the ^1H spin lattice relaxation times. Samples were packed in Delrin rotors and spun at speeds of between 3.0 and 4.0 kHz at the magic angle. A sweep width of 20 kHz with a total acquisition time of 12.8 ms was used. Between 20 and 200 FID's were collected, zero filled to 8 K, and transformed with an experimental line broadening of 10–50 Hz. Chemical shift data are referenced to 85% phosphoric acid.

Crystal Data: $C_{72}H_{60}Br_4Cu_4P_4$, M_r = 1623, orthorhombic, space group *Pbcn* (D_{2h}^{14}, No. 60), a = 17.662 (5) Å, b = 20.748 (7) Å, c = 18.351 (6) Å, V = 6724 (4) Å^3, D_{measd} = 1.61 (1), D_{calcd} (Z = 4) = 1.60 g cm^{-3}, $F(000)$ = 3232; monochromatic Kα radiation, λ = 0.7106$_9$ Å, μ_{Mo} = 39.5 cm^{-1}; prism, 0.10 × 0.10 × 0.42 mm (capillary), T = 295 K. A^*_{min} = 1.31, A^*_{max} = 1.40.

Structure Determination. A unique data set was measured to $2\theta_{max}$ = 50° on a Syntex $P2_1$ four-circle diffractometer in conventional $2\theta/\theta$ scan mode. A total of 5966 independent reflections were obtained, 3708 with $I > 3\sigma(I)$ being considered observed and used in the full-matrix least-squares refinement after analytical absorption correction. Anisotropic thermal parameters were refined for the non-hydrogen atoms; $(x, y, z, U_{iso})_H$ were included constrained at idealized values. Residuals (R, R') at convergence (on $|F|$) were 0.044 and 0.047, reflection weights being $(\sigma^2(F_o) + 0.0005(F_o)^2)^{-1}$. Neutral

(1) (a) Griffith University. (b) University of Western Australia.
(2) Churchill, M. R.; Kalra, K. L. *Inorg. Chem.* **1974**, *13*, 1065.
(3) Churchill, M. R.; Kalra, K. L. *Inorg. Chem.* **1974**, *13*, 1427.
(4) Churchill, M. R.; DeBoer, B. G.; Donovan, D. J. *Inorg. Chem.* **1975**, *14*, 617.
(5) Teo, B.-K.; Calabrese, J. C. *Inorg. Chem.* **1976**, *15*, 2467.
(6) Teo, B.-K.; Calabrese, J. C. *J. Chem. Soc., Chem. Commun.* **1976**, 185.
(7) Teo, B.-K.; Calabrese, J. C. *Inorg. Chem.* **1976**, *15*, 2474.
(8) Goel, R. G.; Beauchamp, A. L. *Inorg. Chem.* **1983**, *22*, 395.
(9) Healy, P. C.; Pakawatchai, C.; Raston, C. L.; Skelton, B. W.; White, A. H. *J. Chem. Soc., Dalton Trans.* **1983**, 1905.
(10) Churchill, M. R.; Youngs, W. J. *Inorg. Chem.* **1979**, *18*, 1133.
(11) Costa, G.; Reisenhofer, E.; Stefani, L. *J. Inorg. Nucl. Chem.* **1965**, *27*, 2581.

0020-1669/84/1323-3766$01.50/0